

Figure S1

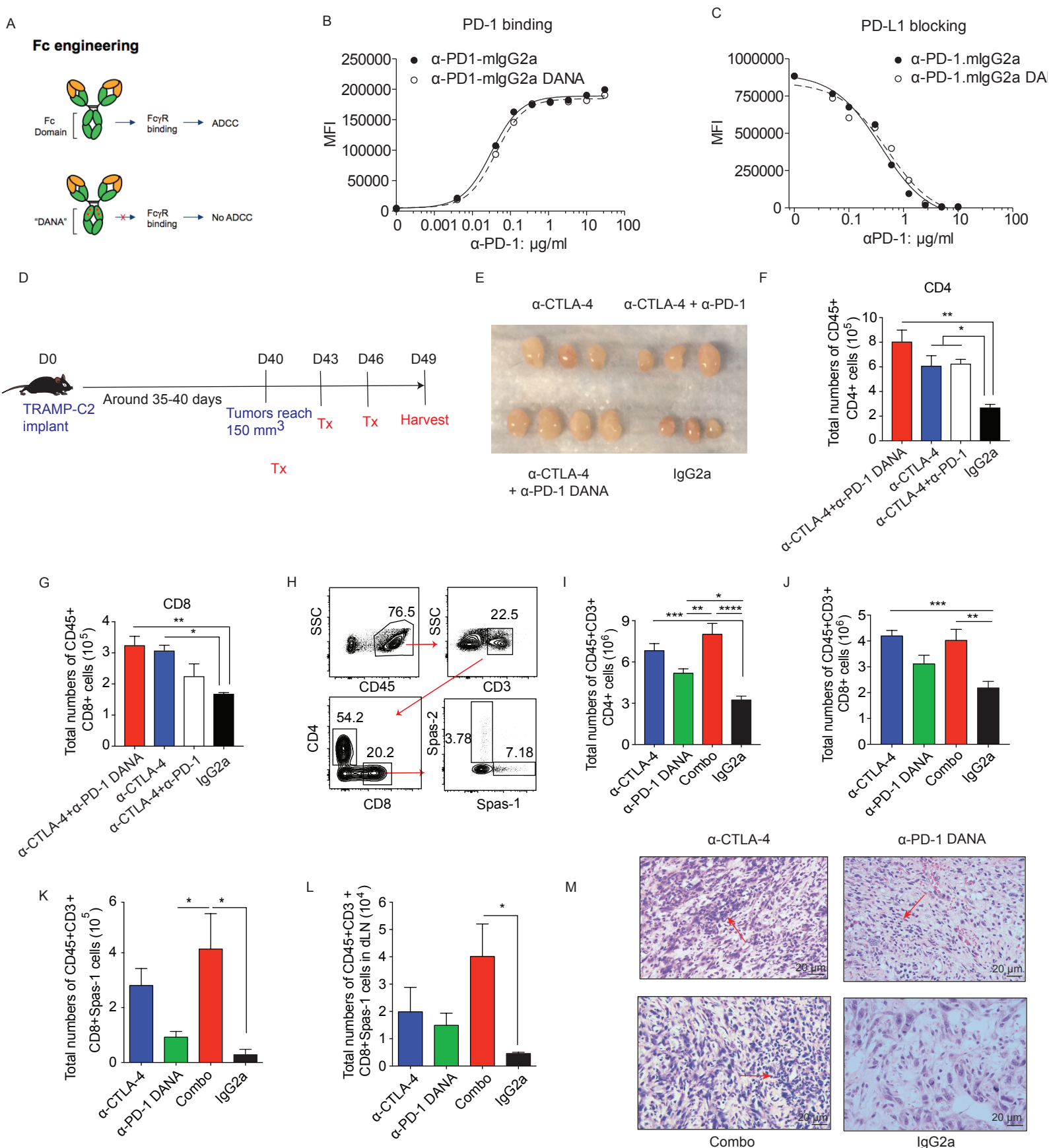


Figure S1. Related to Figure 1. ADCC-mediated depletion of activated CD4⁺ and CD8⁺ T cells and expansion of antigen-specific T cells post checkpoint blockade.

C57BL/6j WT mice were injected with TRAMP-C2 (1×10^6 cells/mouse) in the right flank on day 0 and treated with different checkpoint inhibitors. (A) Illustration of anti-PD-1 and anti-PD-1 DANA monoclonal antibodies. (B) EL4 cells expressing PD-1 were incubated with the indicated PD-1 antibodies followed by secondary detection with anti-mouse IgG. (C) HEK293 cells overexpressing mouse PD-1 were incubated with mouse PD-L1 extracellular domain fused to human IgG1 +/- the indicated PD-1 antibodies followed by secondary detection with anti-human IgG. (D) Schema of animal studies. (E) Pictures of draining lymph nodes harvested on day 49 after different immunotherapy treatments. (F) Total CD4⁺ T cells from draining lymph node (G) Total CD8⁺ T cells from draining lymph nodes. (H-M) Mice were implanted with TRAMP-C2 on day 0 and treated with checkpoint inhibitors on day 40, 43, 46 and harvested on day 49. (H) Flow gating strategy of antigen-specific T cells. (I) Total numbers of CD4⁺ T cells in spleens. (J) Total numbers of CD8⁺ T cells in spleens (K) Total numbers of CD8⁺Spas-1 T cells in spleens. (L) Total numbers of CD8⁺Spas-1 T cells in draining lymph nodes. (M) Representative H&E staining from tumor samples harvested three days after the last treatment. Data from H-M were collected from 8 mice per group from two independent experiments. Statistics were analyzed by one-way ANOVA with post-hoc Tukey test. (*) $P < 0.05$, (**) $P < 0.01$, (***) $P < 0.001$, (****) $P < 0.0001$.

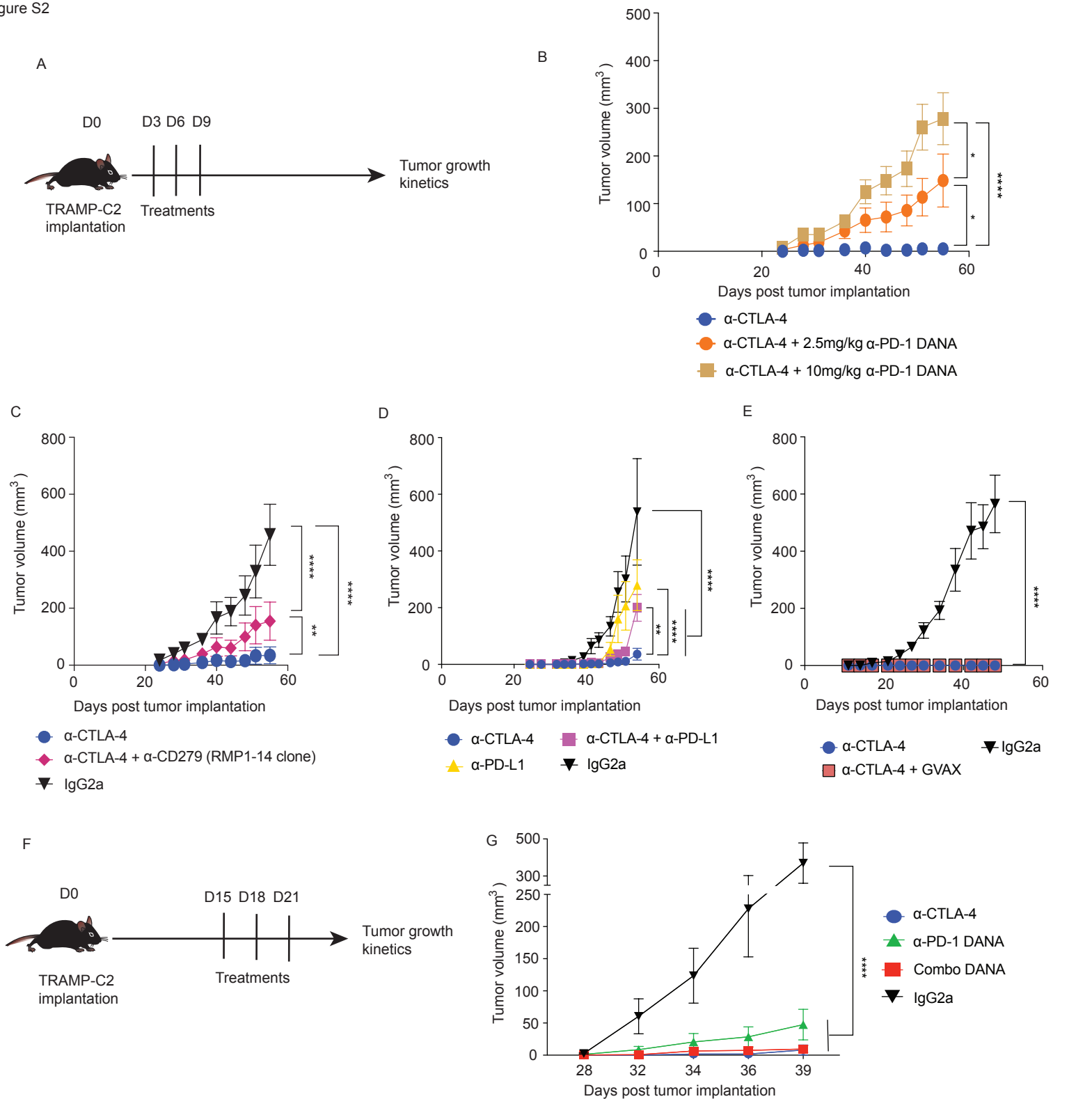


Figure S2. Related to Figure 2. Different combination immunotherapies in the TRAMP-C2 tumor model.

(A) Mice were implanted with TRAMP-C2 on day 0 and treated with different combination immunotherapies at day 3, 6, and 9. Mice were monitored for tumor growth. (B) Tumor growth with two different doses of anti-PD-1 DANA antibody combined with anti-CTLA-4 blockade. The doses of anti-PD-1 DANA are 2.5 mg/kg and 10 mg/kg. (C) Different clones of anti-PD1 antibody and their respective anti-tumor effects. The dose for each checkpoint inhibitor is 10 mg/kg. For (B) and (C), data were collected from two independent experiments with 8 mice per group. (D) Mice were treated with anti-CTLA-4, anti-PD-L1, combination treatment or isotype control. Figure demonstrated the tumor growth curves. Data were collected from 7 mice per group. (E) Tumor growth curves of combination of CTLA-4 blockade with GVAX vaccine. The dose for anti-CTLA-4 is 10 mg/kg. The dose for GVAX vaccine is 10^6 irradiated cells. Data were collected from 10 mice per group. (F) Mice were implanted with TRAMP-C2 on day 0 and treated with different combination immunotherapies at day 15, 18, and 21. (G) Tumor growth curves among different treatments. Data were collected from 8 mice per group. Statistics were analyzed by two-way ANOVA with post-hoc test. (*) $P < 0.05$, (**) $P < 0.01$, (***) $P < 0.001$, (****) $P < 0.0001$.

Figure S3

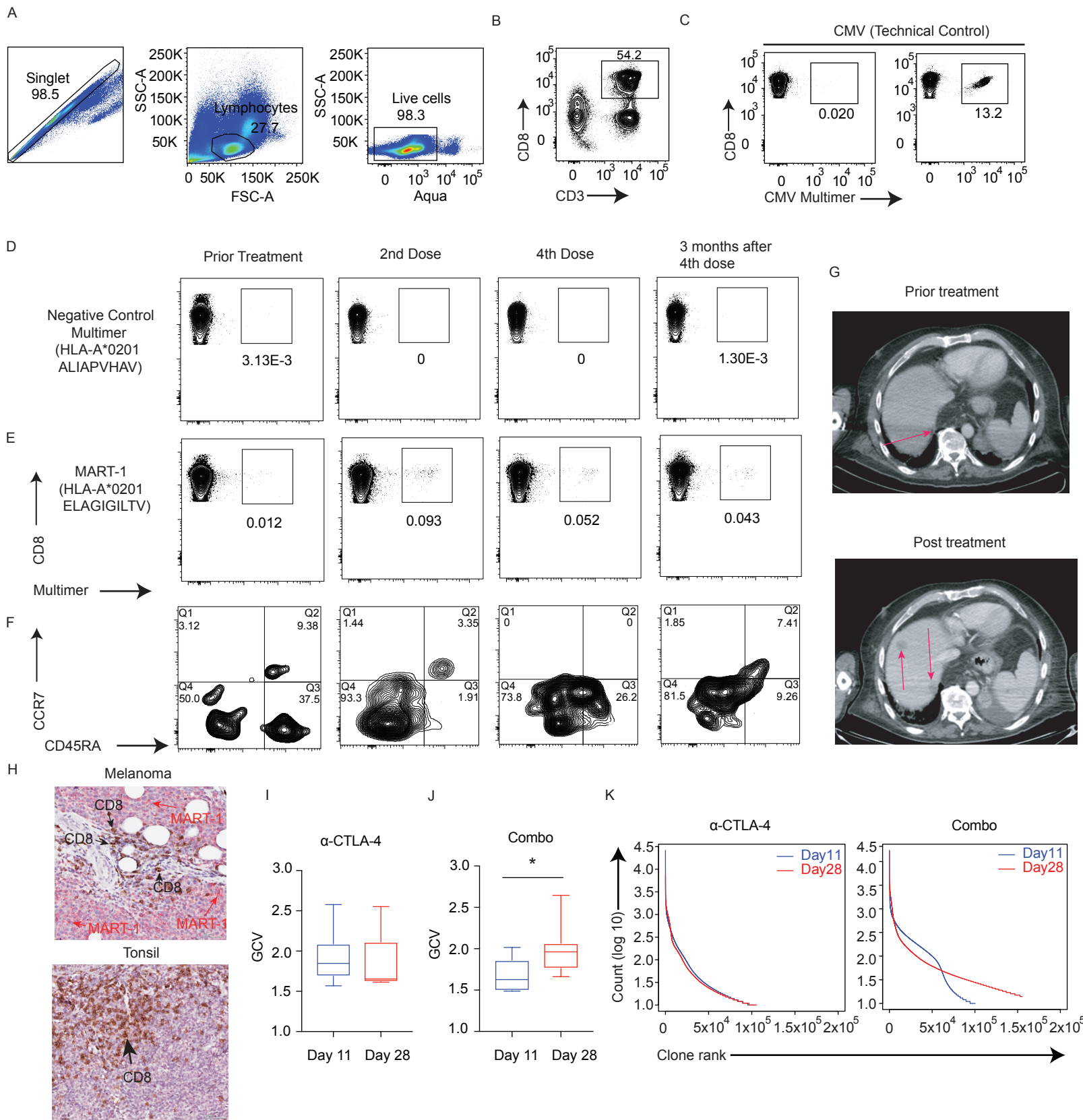


Figure S3. Related to Figure 3. The loss of MART-1 specific CD8+ T cells post combination checkpoint blockade treatment in a metastatic melanoma patient is associated with poor clinical outcome in the low disease state and the dynamics of TCR clonotypes post checkpoint inhibition in mice.

A treatment-naïve patient with metastatic melanoma underwent debulking surgery and then received four doses of ipilimumab plus nivolumab at a three week interval, followed by maintenance with nivolumab. PBMCs were collected from different time points, including baseline (without any treatment), after two cycles of ipilimumab with nivolumab treatments, and three months after the 4th cycle of ipilimumab and nivolumab. (A-B) Flow gating strategy is shown. After pre-gating with Aqua-CD45+CD3+CD8+, cells were analyzed with multimers. (C) This patient is CMV negative as shown in the left panel. We used another CMV+ donor as a positive control. (D-E) After pre-gating with Aqua- CD45+CD3+CD8+, cells were analyzed by MART-1 expression with either negative control multimer (ALIAPVHAV) or MART-1 multimer (ELAGIGILTV). (F) MART-1 positive cells were further gated on CCR7 and CD45RA. (G) The clinical response of the patient post combination treatment. (H) Immunohistochemistry for CD8 (brown) and MART-1 (red) was performed on the melanoma tissue derived from this patient and on control tonsil tissue. The tonsil tissue was used as a negative control for MART-1 staining. For I-K, mice were implanted with TRAMP-C2 on day 0 and treated with checkpoint inhibitors on day 3, 6, 9. Tumor-draining lymph nodes were harvested on day 11 and day 28 for subsequent TCR analysis. (I-J) Geometric Coefficient Variation (GCV) plots of TCR sequence diversity. (K) To assess the frequency distributions of T cell clones, TCR clone abundance was ranked in descending order from anti-CTLA-4 and combo treated mice on day 11 and day 28. Data were collected from 7 mice per group. Two-tailed Student's t-test was used to calculate statistical difference. (*)P<0.05

Figure S4

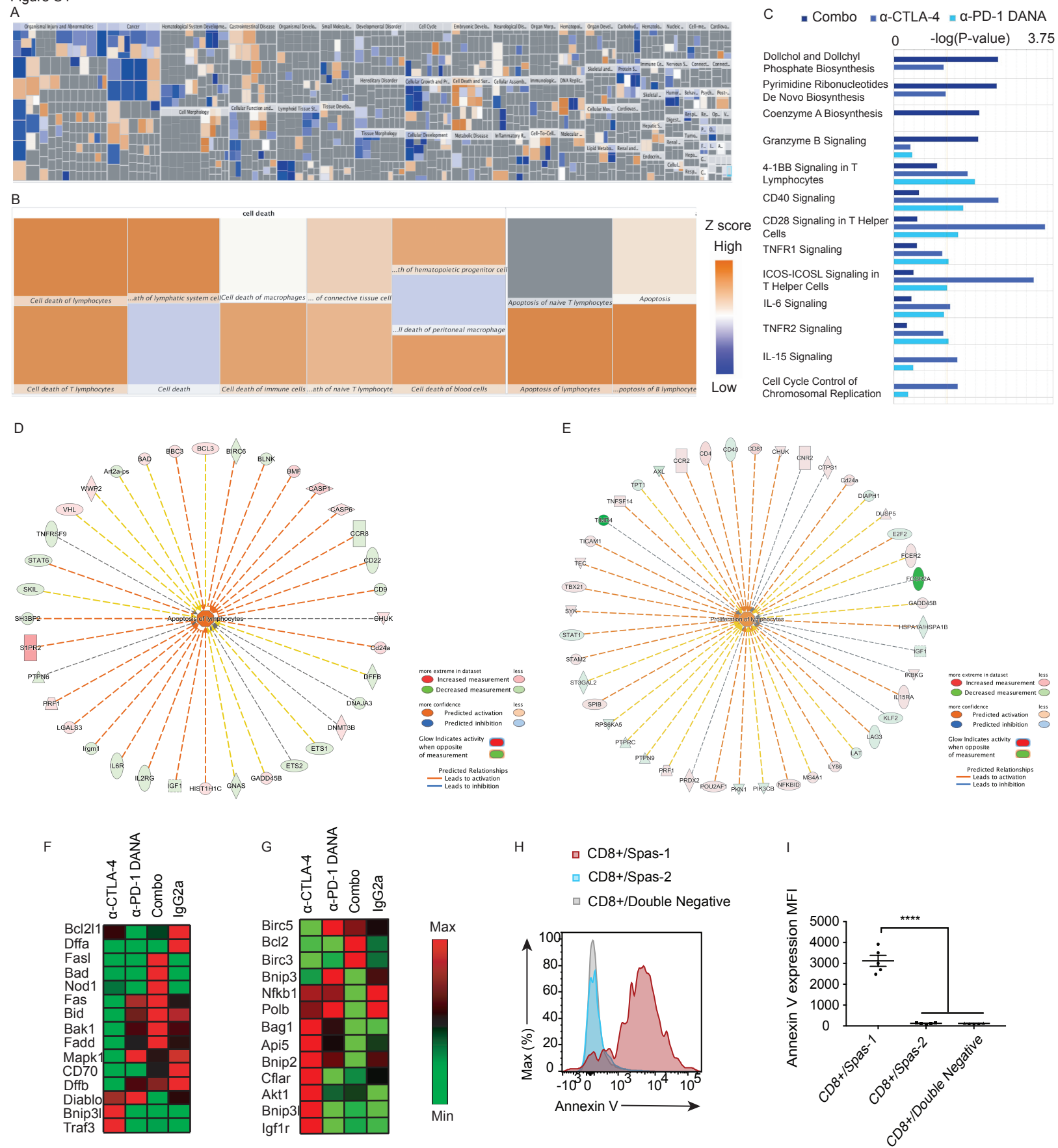


Figure S4. Related to Figure 4. Ingenuity pathway analysis (IPA) and differential gene expression among checkpoint inhibitor treated groups. Mice were implanted with TRAMP-C2 tumors and treated with different checkpoint inhibitors. Spas-1 CD8⁺ T cells were sorted, and RNA was extracted for subsequent RNA sequence analysis. (A) IPA analysis of different pathways from the combination treated groups. (B) Gene clusters in cell death and apoptosis pathways from the combination treated group. (C) Differential pathway analysis was performed between the different treatment groups. (D) The highest ranked pathway for combination treated group was the cell death pathway. (E) The highest ranked pathway for the anti-CTLA-4 treated group was lymphocyte proliferation. (F) Gene expression of pro-apoptotic gene clusters was assessed using RT-PCR. (G) Gene expression for anti-apoptotic transcripts was assessed using RT-PCR. (H-I) Splenocytes were isolated from tumor-bearing mice treated with checkpoint blockade at day 3, 6, 9 post TRAMP-C2 implantation. (H) Annexin V expression among Spas-1, Spas-2, or MHC/peptide multimer negative CD8⁺ T cells. (I) MFI expression levels of Annexin V in different CD8 subsets. Statistical analyses were calculated by one-way ANOVA or with post-hoc Tukey test. (****)P<0.0001

Figure S6

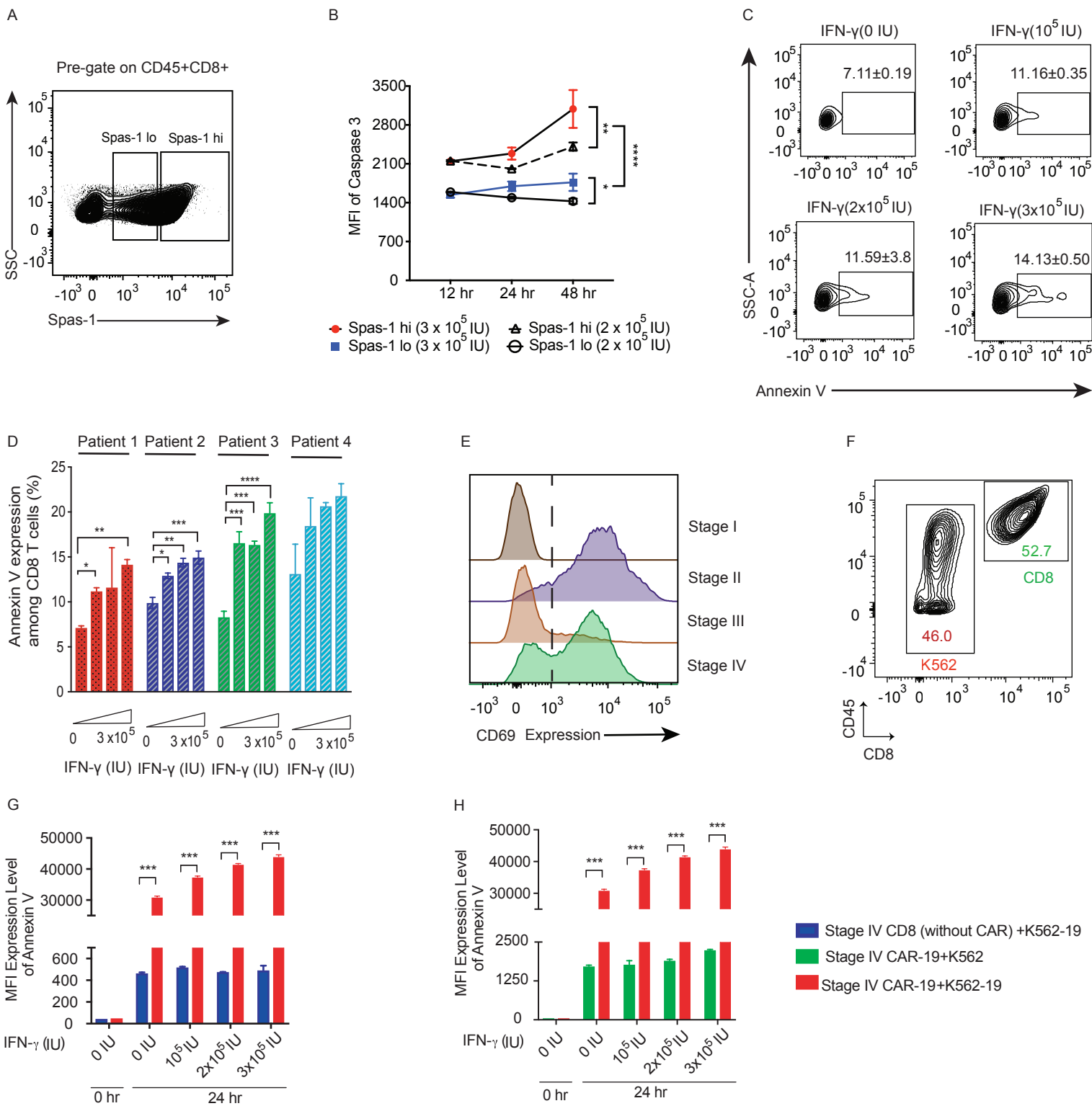


Figure S6. Related to Figure 5. T cell apoptosis induced by IFN- γ

(A) Splenocytes were harvested from TRAMP-C2 bearing mice. Gating strategies of Spas-1hi and Spas-1lo CD8 T cell clones. (B) Caspase-3 expression among different CD8+ Spas-1 subsets at different time points. Data were collected from 5 mice per group. (C-D) Peripheral blood mononuclear cells (PBMC) from nivolumab-treated patients with metastatic melanoma were stimulated *in vitro* with different concentrations of IFN- γ and harvested 48 hours later. Annexin V expression in CD8+ T cell subsets after stimulation with different concentration of IFN- γ . Data described as mean \pm SEM. (E) CD69 expression among different stages of CD8+ T cells. (F) Stage IV T cells or untransfected CD8+ T cells were co-cultured with either WT K-562 cancer cells or CD19 ligand expressing K-562 cells at 1:1 ratio. Cells were harvested 48 hours after co-culture. Figure demonstrates the flow gating strategy between K-562 and CD8 T cells. (G-H) Stage IV T cells were co-cultured with either K-562 or K562-19 cancer cells under different concentrations of human recombinant IFN- γ protein. Annexin V expression was analyzed by flow cytometry. Statistical analyses were calculated by either one-way ANOVA or two-way ANOVA with post-hoc Tukey test. (*)P<0.05, (**)P<0.01, (***)P<0.001, (****)P<0.0001

Figure S7

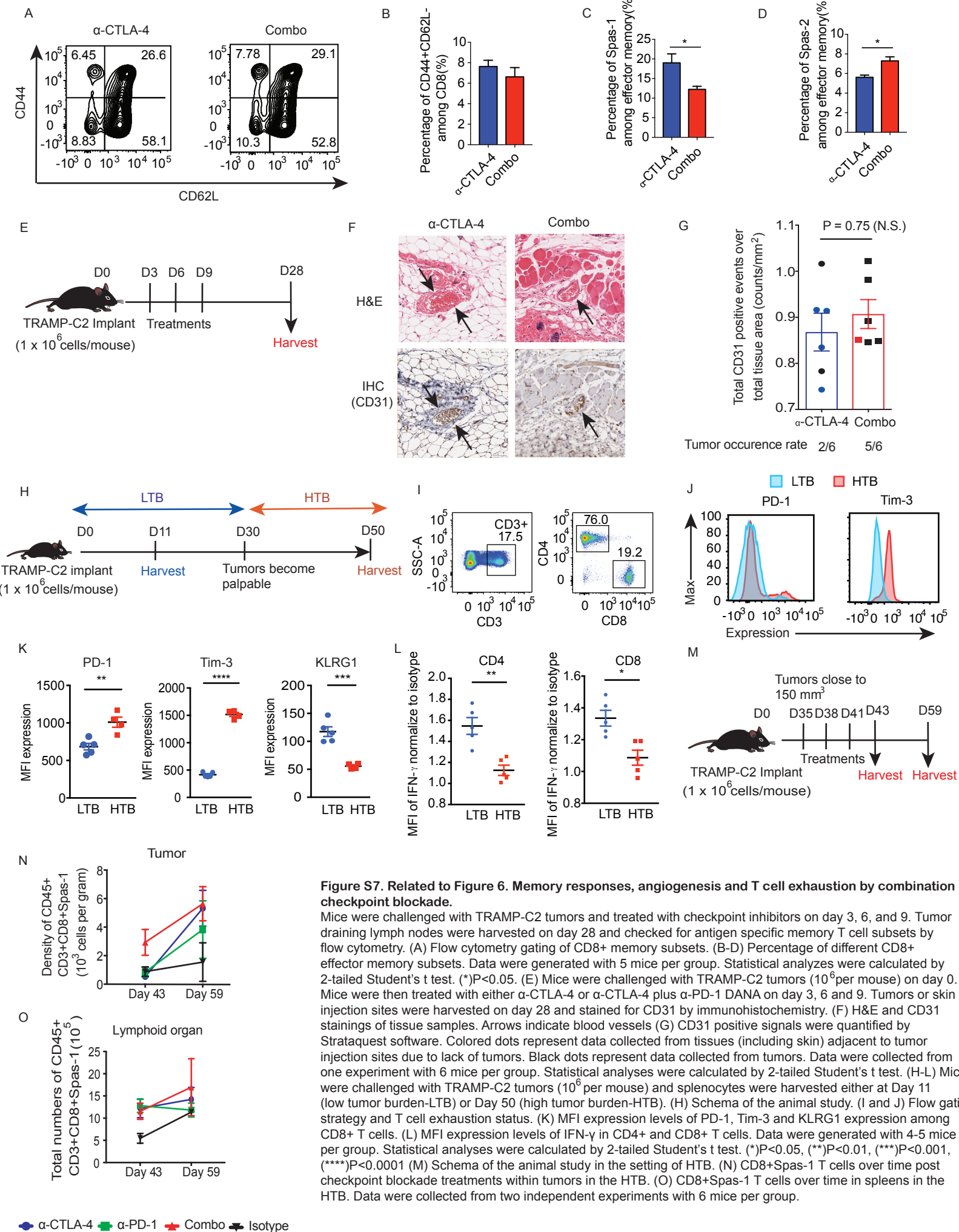
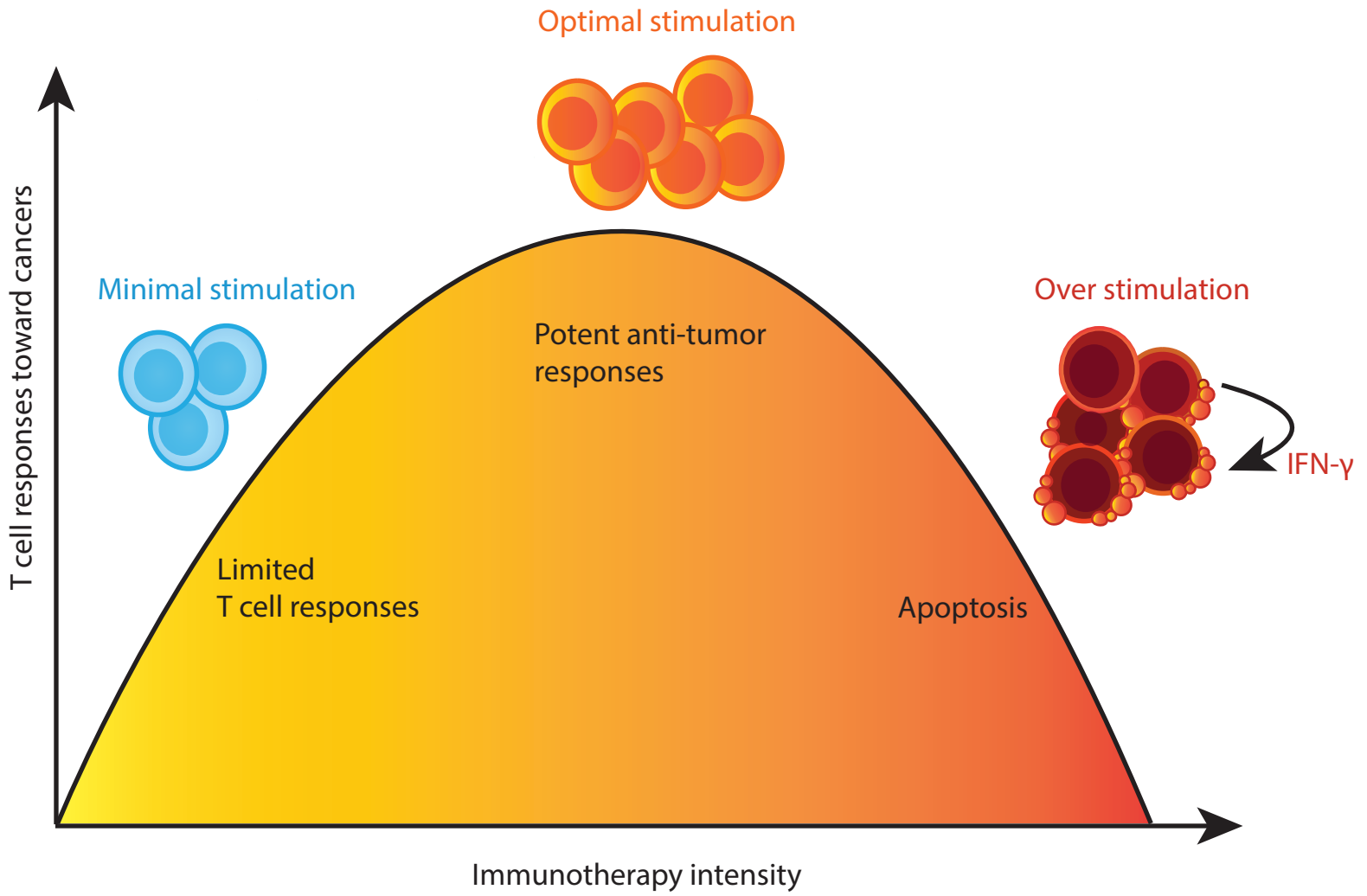


Figure S7. Related to Figure 6. Memory responses, angiogenesis and T cell exhaustion by combination checkpoint blockade.

Mice were challenged with TRAMP-C2 tumors and treated with checkpoint inhibitors on day 3, 6, and 9. Tumor draining lymph nodes were harvested on day 28 and checked for antigen specific memory T cell subsets by flow cytometry. (A) Flow cytometry gating of CD8+ memory subsets. (B-D) Percentage of different CD8+ effector memory subsets. Data were generated with 5 mice per group. Statistical analyses were calculated by 2-tailed Student's t test. (*)P<0.05. (E) Mice were challenged with TRAMP-C2 tumors (10^6 per mouse) on day 0. Mice were then treated with either α -CTLA-4 or α -CTLA-4 plus α -PD-1 DANA on day 3, 6 and 9. Tumors or skin injection sites were harvested on day 28 and stained for CD31 by immunohistochemistry. (F) H&E and CD31 stainings of tissue samples. Arrows indicate blood vessels (G) CD31 positive signals were quantified by Strataquest software. Colored dots represent data collected from tissues (including skin) adjacent to tumor injection sites due to lack of tumors. Black dots represent data collected from tumors. Data were collected from one experiment with 6 mice per group. Statistical analyses were calculated by 2-tailed Student's t test. (H-L) Mice were challenged with TRAMP-C2 tumors (10^6 per mouse) and splenocytes were harvested either at Day 11 (low tumor burden-LTB) or Day 50 (high tumor burden-HTB). (H) Schema of the animal study. (I and J) Flow gating strategy and T cell exhaustion status. (K) MFI expression levels of PD-1, Tim-3 and KLRG1 expression among CD8+ T cells. (L) MFI expression levels of IFN- γ in CD4+ and CD8+ T cells. Data were generated with 4-5 mice per group. Statistical analyses were calculated by 2-tailed Student's t test. (*)P<0.05, (**)P<0.01, (***)P<0.001, (****)P<0.0001 (M) Schema of the animal study in the setting of HTB. (N) CD8+Spas-1 T cells over time post checkpoint blockade treatments within tumors in the HTB. (O) CD8+Spas-1 T cells over time in spleens in the HTB. Data were collected from two independent experiments with 6 mice per group.



Goldilocks phenomena of checkpoint inhibitor blockade. Related to the abstract figure

Our results indicate while insufficient immune stimuli fail to protect against tumor growth (PD-1 blockade in our mice experiments), exceeding an immune stimulatory threshold, particularly in the LTB, may trigger an immunomodulatory regulation mechanism that suppresses anti-tumor responses via IFN- γ . Achieving the optimal magnitude of immune stimulation may be critical for successful immunotherapy strategies and achieving optimal tumor control as well as long-term outcome for patients.

Table S1. Patient demographics and disease characteristics in advanced melanoma patients by treatments. Related to Figure 3.

Characteristics	Mono-treated	Combo-treated
Median age – years (range)	63 (19-90)	63 (24-85)
Sex – no. (%)		
• Male	65 (65)	34 (64.2)
• Female	35 (35)	19 (35.8)
Primary site – no. (%)		
• Acral	0 (0)	3 (6.8)
• Cutaneous	76 (80)	32 (72.7)
• Mucosal	8 (8.4)	4 (9.1)
• Uveal	11 (11.6)	5 (11.4)
• Missing	5 (5)	9 (17)
Stage – no. (%)		
• IIIC	1 (1)	7 (13.2)
• IV (M1a)	19 (19)	6 (11.3)
• IV (M1b)	29 (29)	5 (9.4)
• IV (M1c)	51 (51)	35 (66)
Baseline LDH – no. (%)		
• Normal (\leq ULN)	61 (61.6)	29 (54.7)
• Elevated ($>$ ULN)	38 (38.4)	21 (39.6)
• Missing	1 (1)	3 (5.7)
Mean Baseline Tumor Size – cm (range)	10.5 (1-40.7)	9.5 (1-37.1)
BRAF status		
• WT	79 (79)	32 (61.5)
• V600 mutation	18 (18)	15 (28.8)
• Other	3 (3)	5 (9.6)
• Missing	0 (0)	1 (1.9)
ECOG – no. (%)		
• 0-1	100 (100)	51 (96.2)
• \geq 2	0 (0)	2 (3.8)
Liver met – no. (%)		
• No	66 (66)	31 (58.5)
• Yes	34 (34)	22 (41.5)
Lung met – no. (%)		
• No	51 (51)	30 (56.6)
• Yes	49 (49)	23 (43.4)
Brain met – no. (%)		
• No	82 (82)	37 (69.8)
• Yes	18 (18)	16 (30.2)

Table S2. In vivo injection antibodies. Related to STAR METHODS.

Name	Clone	Dosage (mg per kg /injection /mouse)	Company
Anti-CTLA-4	UC-10	2.5-10	AbbVie
Anti-PD-1	17D2	10	AbbVie
Anti-PD-1	RMP1-14	10	BioXCell
Anti-PD-1 DANA	17D2	2.5-10	AbbVie
Anti-PD-L1	10F.9G2	10	BioXCell

Note:

1. BioXCell anti-PD-1 was used in Figure 3D for comparison. All other anti-PD-1/
anti-PD-1 DANA monoclonal antibodies used in this manuscript were provided
by AbbVie.

Table S3. Antibodies used in flow cytometry. Related to STAR METHODS.

Markers	Company	Cat No.	Clone	Florescence	Note
CD3	Biologend	100232	17A2	BV785	
CD4	Biologend	100447	GK1.5	BV711	
CD8	BD Bioscience	552877	53-6.7	PE-Cy7	
CD16/32	TONBO	70-0161-U500	2.4G2	N/A	Fc block
CD44	Biologend	103049	IM7	BV650	
CD45	Biologend	103126	30-F11	PB	
CD45.1	Biologend	110737	A20	BV605	
CD45.2	Biologend	109847	104	BV711	
CD62L	Biologend	104433	MEL-14	BV570	
Foxp3	eBioscience	11-5773-82	FJK-16s	FITC	
rlgG2a/k	eBioscience	11-4321	eBR2a	FITC	Isotype
PD-1	Biologend	135213	29F.1A12	FITC	
rlgG2a/k	Biologend	400505	RTK2758	FITC	Isotype
Tim-3	Biologend	134003	B8.2C12	PE	
rlgG1/k	Biologend	400407	RTK2071	PE	Isotype
KLRG1	Biologend	138412	2F1	APC	
Hamster IgG	Biologend	402012	N/A	APC	Isotype
IFN- γ	BD Bioscience	554411	XMG1.2	FITC	
Rat IgG1	BD Bioscience	553924	R3-34	FITC	Isotype
CD119	BD Bioscience	740897	GR20	BV786	
Rat IgG2a	BD Bioscience	563335	R35-95	BV786	Isotype
Caspase-3	BD Bioscience	51-68654X	N/A	FITC	Apoptosis
Annexin V	BD Bioscience	51-65874X	N/A	FITC	Apoptosis
Spas-1	NIH tetramer Core	N/A	N/A	PE	Sequence: STHVNHLHC H-2D(b)
Spas-2	NIH tetramer Core	N/A	N/A	APC	Sequence: IIITFNDL H-2K(b)

Table S4. Antibodies used in Cy-TOF. Related to STAR METHODS.

Markers	FLDM#	Clone
CD45	3089003B	HI30
CD11c	BL337202	Bu15 (Custom order)
CD235ab/CD61	BL306602/BL336402	HIR2/V1-PL2 (Custom order)
CD16	BL 302002	3G8 (Custom order)
CD45RA	3143006B	HI100
CD4	3145001B	RPA-T4
CD8a	3146001B	RPA-T8
BDCA-2	3147009B	201A
CD14	3151009B	M5E2
FoxP3	3162011A	PCH101
CD25	3169003B	2A3
IFN- γ	3165002B	B27
CD127 (IL-7Ra)	3168017B	A019D5
CD3	3170001B	UCHT1
HLA-DR	3174001B	L243
CD56	3176008B	NCAM16.1
CD27	3167006B	L128
gdTCR	BL331202	B1(Custom order)
TCRVd2	BL331402	B6 (Custom order)

* BL indicate antibodies from Biolegend and customized.

Table S5. Primers for RNA sequencing. Related to STAR METHODS.

Name	Sequence	Direction
Biotin-TSOLNA	/5Biosg/AAGCAGTGGTATCAACGCAGAGTACATrGrG+G	Forward
Biotin-Oligo-dT30VN	/5Biosg/AAGCAGTGGTATCAACGCAGAGTACT30VN	Reverse
Biotin-ISPCR oligo	/5Biosg/AAGCAGTGGTATCAACGCAGAGT	Both
read1_bc_1_GAGT AG	AATGATACGGCGACCACCGAGATCTACACGAGGTAGTCGTCGGCAGCGTCA GATGTGTATAAGAGACAG	Forward
read1_bc_2_GCTTA AC	AATGATACGGCGACCACCGAGATCTACACGCTTAACTCGTCGGCAGCGTCA GATGTGTATAAGAGACAG	Forward
read1_bc_3_GCAAT TC	AATGATACGGCGACCACCGAGATCTACACGCAATTCTCGTCGGCAGCGTCA GATGTGTATAAGAGACAG	Forward
read1_bc_13_GATC CTA	AATGATACGGCGACCACCGAGATCTACACGATCCTATCGTCGGCAGCGTCA GATGTGTATAAGAGACAG	Forward
read1_bc_14_TGGT CTC	AATGATACGGCGACCACCGAGATCTACACTGGTCTCTCGTCGGCAGCGTCA GATGTGTATAAGAGACAG	Forward
read1_bc_15_TCCA GTC	AATGATACGGCGACCACCGAGATCTACACTCCAGTCTCGTCGGCAGCGTCA GATGTGTATAAGAGACAG	Forward
read1_bc_25_ACAC TTG	AATGATACGGCGACCACCGAGATCTACACACACTTGTCTCGTCGGCAGCGTCA GATGTGTATAAGAGACAG	Forward
read1_bc_26_TACG GCA	AATGATACGGCGACCACCGAGATCTACACTACGGCATCGTCGGCAGCGTCA GATGTGTATAAGAGACAG	Forward
read1_bc_27_TCTC GTG	AATGATACGGCGACCACCGAGATCTACACTCTCGTGTCTCGTCGGCAGCGTCA GATGTGTATAAGAGACAG	Forward
read1_bc_37_GTCA TCC	AATGATACGGCGACCACCGAGATCTACACGTCATCCTCGTCGGCAGCGTCA GATGTGTATAAGAGACAG	Forward
read1_bc_38_ACCG TAC	AATGATACGGCGACCACCGAGATCTACACACCGTACTCGTCGGCAGCGTCA GATGTGTATAAGAGACAG	Forward
read1_bc_39_GTAC TAC	AATGATACGGCGACCACCGAGATCTACACGTAATACTCGTCGGCAGCGTCA GATGTGTATAAGAGACAG	Forward
read2_bc_1_GACGT AC	CAAGCAGAAGACGGCATAACGAGATGACGTACGTCTCGTGGGCTCGGAGAT GTGTATAAGAGACAG	Reverse
read2_bc_2_AACTG CA	CAAGCAGAAGACGGCATAACGAGATAACTGCAGTCTCGTGGGCTCGGAGAT GTGTATAAGAGACAG	Reverse
read2_bc_3_CCACA GT	CAAGCAGAAGACGGCATAACGAGATCCACAGTGTCTCGTGGGCTCGGAGAT GTGTATAAGAGACAG	Reverse
read2_bc_13_GGTC CTA	CAAGCAGAAGACGGCATAACGAGATGGTCCTAGTCTCGTGGGCTCGGAGAT GTGTATAAGAGACAG	Reverse
read2_bc_14_CCAA CGA	CAAGCAGAAGACGGCATAACGAGATCCAACGAGTCTCGTGGGCTCGGAGAT GTGTATAAGAGACAG	Reverse
read2_bc_15_AGGA CAC	CAAGCAGAAGACGGCATAACGAGATAGGACAGTCTCGTGGGCTCGGAGAT GTGTATAAGAGACAG	Reverse
read2_bc_25_GTGT GTC	CAAGCAGAAGACGGCATAACGAGATGTGTGTCTCGTCTCGTGGGCTCGGAGAT GTGTATAAGAGACAG	Reverse
read2_bc_26_GCTA CAA	CAAGCAGAAGACGGCATAACGAGATGCTACAAGTCTCGTGGGCTCGGAGAT GTGTATAAGAGACAG	Reverse
read2_bc_27_CGTA GAC	CAAGCAGAAGACGGCATAACGAGATCGTAGACGTCTCGTGGGCTCGGAGAT GTGTATAAGAGACAG	Reverse
read2_bc_37_CATG GAT	CAAGCAGAAGACGGCATAACGAGATCATGGATGTCTCGTGGGCTCGGAGAT GTGTATAAGAGACAG	Reverse
read2_bc_38_CTGC GAA	CAAGCAGAAGACGGCATAACGAGATCTGCGAAGTCTCGTGGGCTCGGAGAT GTGTATAAGAGACAG	Reverse
read2_bc_39_GAGA CGA	CAAGCAGAAGACGGCATAACGAGATGAGACGAGTCTCGTGGGCTCGGAGAT GTGTATAAGAGACAG	Reverse
Biotin-TSOLNA	/5Biosg/AAGCAGTGGTATCAACGCAGAGTACATrGrG+G	Forward